Magnetar Magnetospheres under the Microscope

Matthew G. Baring
Rice University

(with Zorawar Wadiasingh,
Peter L. Gonthier and Alice K. Harding)

Seminar, School of Physics, University of Melbourne, 6th March, 2019

Giant Spinning Magnets Slowing Down

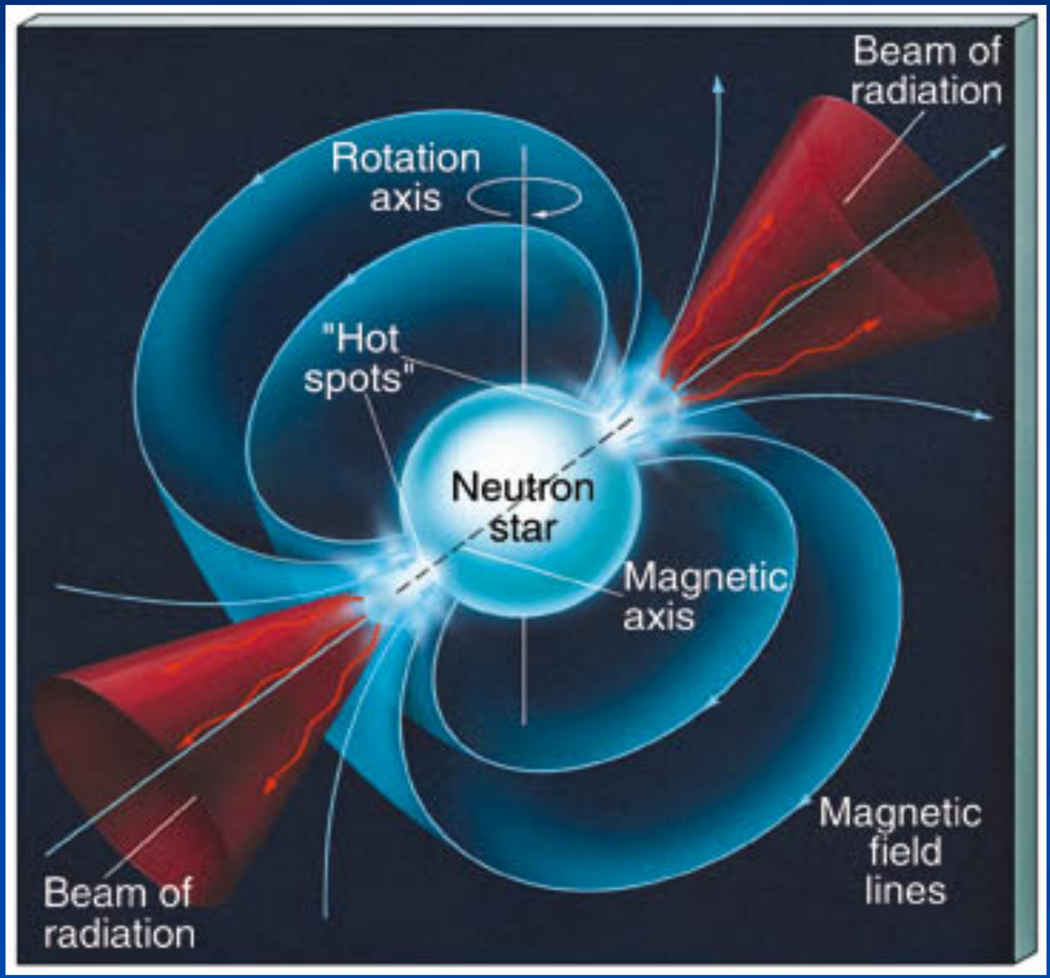

Isolated Pulsar P-Pdot Diagram: *Fermi* era

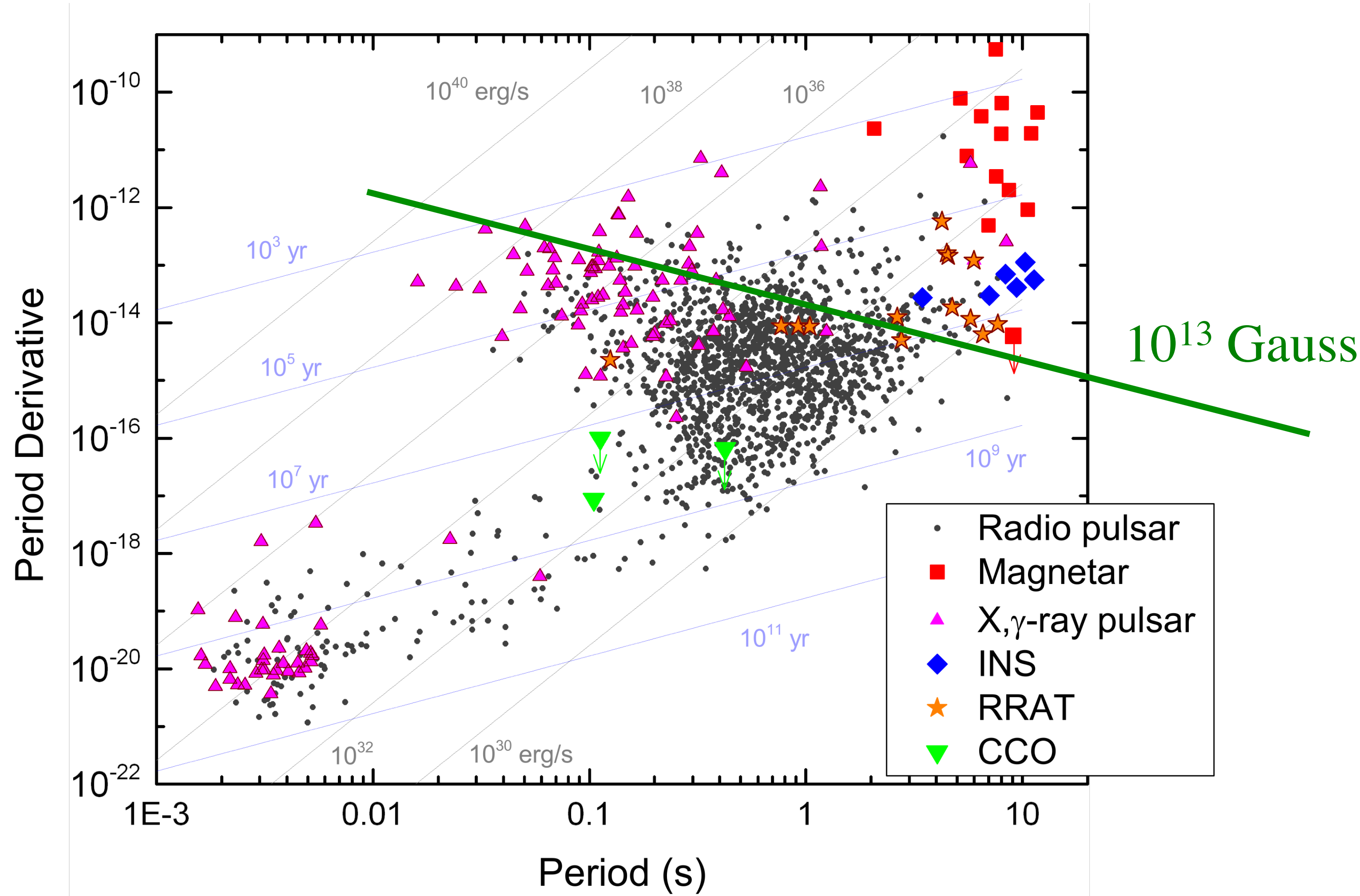

- The phase-space plot for the pulsar population. Dipole field strength B_p inferences scale as the observable $(P\ \mathrm{Pdot})^{1/2}$. Nearly 30 magnetars.

SGR J1550−5418 Bursts January 2009

- *Top*: joint spectra with two BB fit and residuals;
- *Bottom*: Light curves for GBM-NaI (top) and Swift XRT (bottom).
- Lin et al. (ApJ, 2012)

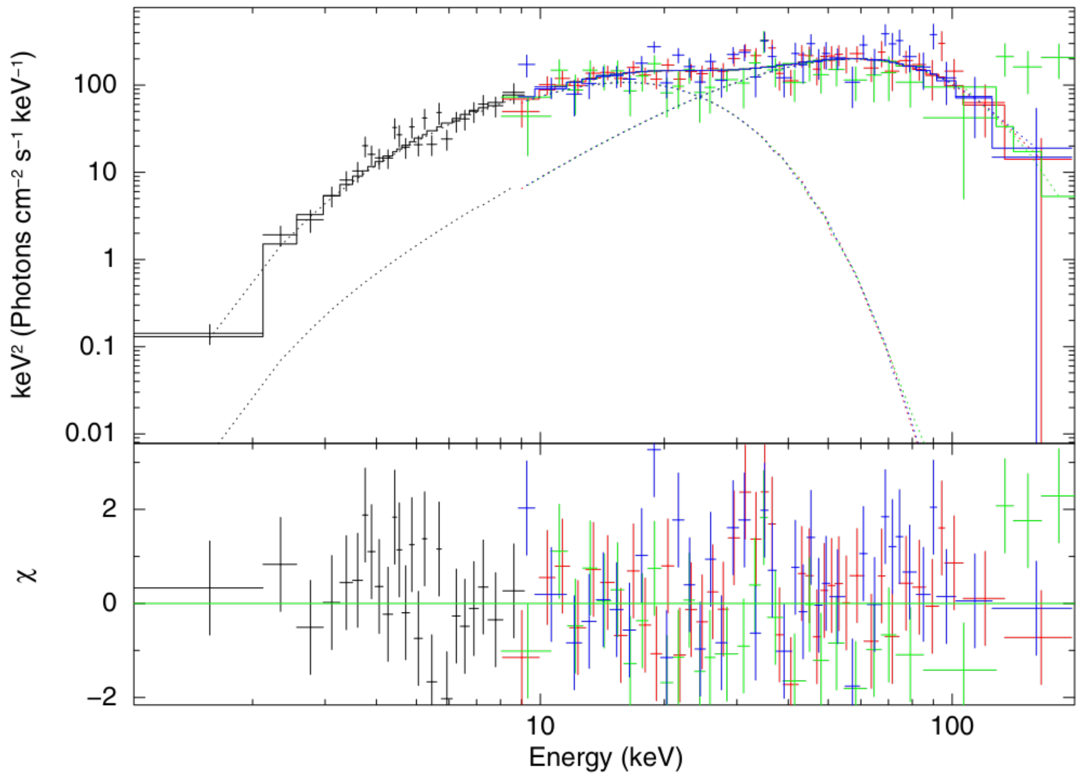

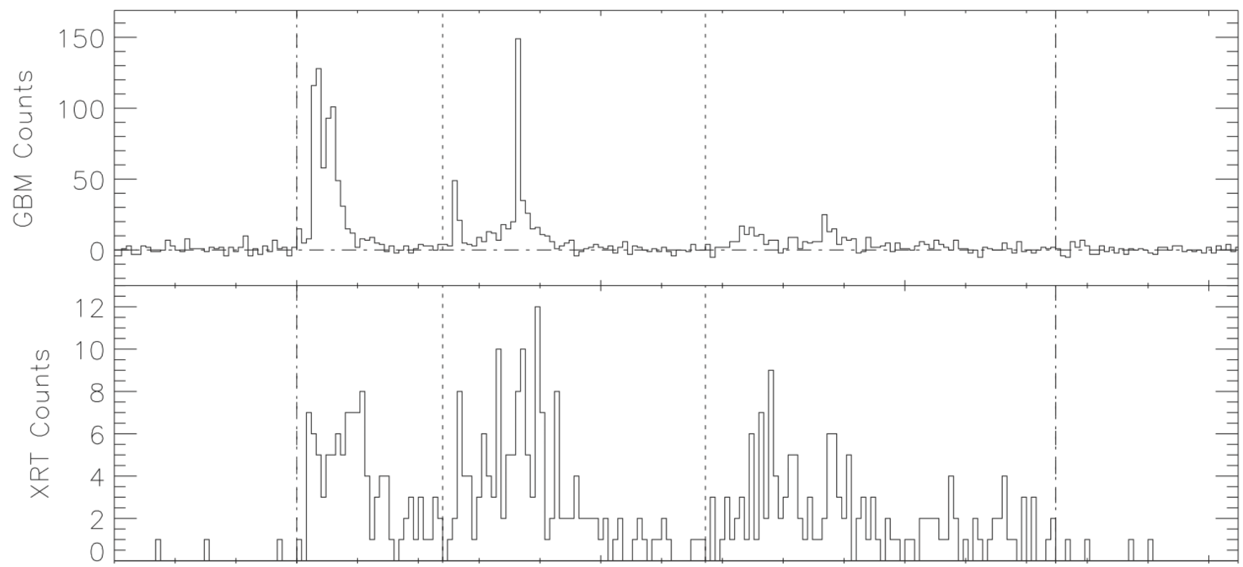

SGR1900+14 Giant Flare Lightcurve

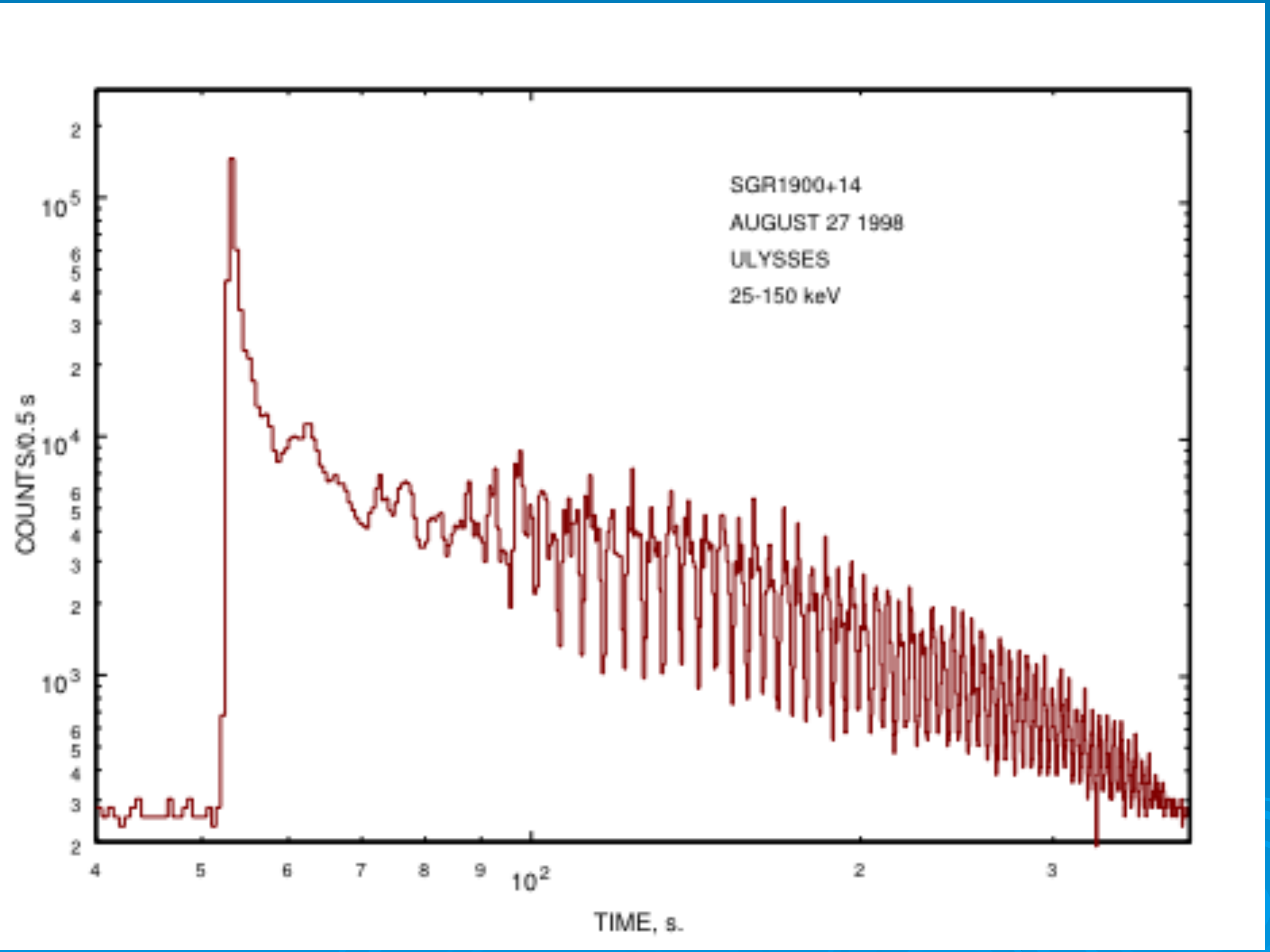

Source: Kevin Hurley

Duncan & Thompson magnetar flare model

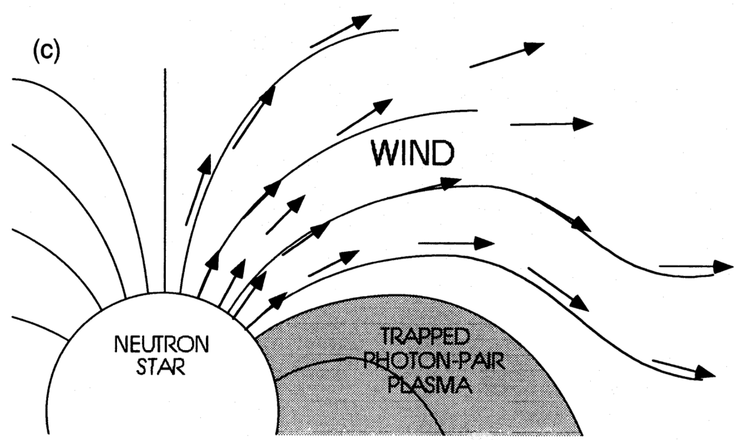

Figure 1. (c) Not all the energy can be contained by the magnetosphere at radius R_ν, unless the total energy released is a very small fraction of the dipole magnetic energy of the star. As a result, the pressure of the photon-pair plasma drives a wind from the magnetosphere. This probably occurred in the 1979 March 5 event, but probably not in most ordinary SGR events.

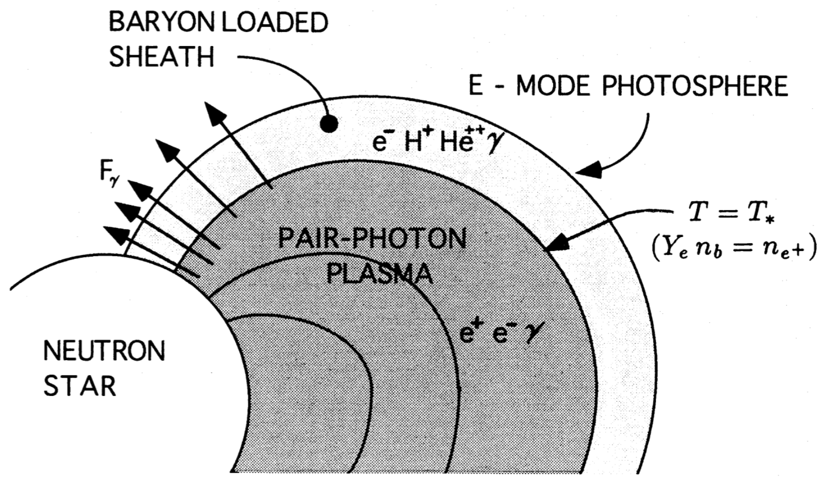

Figure 2. The deposition of $\gtrsim 10^{38}$–10^{41} erg in the magnetosphere of a neutron star is sufficient to generate an optically thick photon–electron–positron plasma. The surface of this plasma is congruent with the magnetic field lines. The surface layers lose heat by radiative diffusion, and the scattering opacity in these layers is dominated by a small contaminant of ions and electrons blown off the neutron star surface.

Magnetars: Hard X-ray Tail Sources

- INTEGRAL, RXTE, NuSTAR etc. have detected hard, non-thermal pulsed tails in nine magnetars (see Table). In all of these, the differential spectra above 20 keV are extremely flat:
  - 1E 1841-045 (Kuiper, Hermsen & Mendez 2004) has a power-law energy index of Γ_h=0.94 between around 20 keV and 150 keV;
  - 4U 0142+61 displays an index of Γ_h=0.2 in the 20 - 50 keV band, with a steepening at higher energies (Kuiper et al. 2006; den Hartog et al. 2008a);
  - RXS J1708-4009 has a Γ_h=0.88 tail in 20-150 keV (detailed in Kuiper et al. 2006; den Hartog et al. 2008b) - see the spectrum on subsequent page.

INTEGRAL/RXTE Spectrum for AXP 1RXJS J1708-4009

Den Hartog et al. (2008)

- XMM spectrum below 10 keV dominates pulsed RXTE/PCA spectrum (black crosses);
- RXTE-PCA (blue) + RXTE-HEXTE (acqua) and INTEGRAL-ISGRI (red) spectrum in 20-150 keV band *is not totally pulsed,* with E^{-1}.
- COMPTEL upper limits *imply spectral turnover around 300-500 keV*, indicated by logparabolic guide curve.

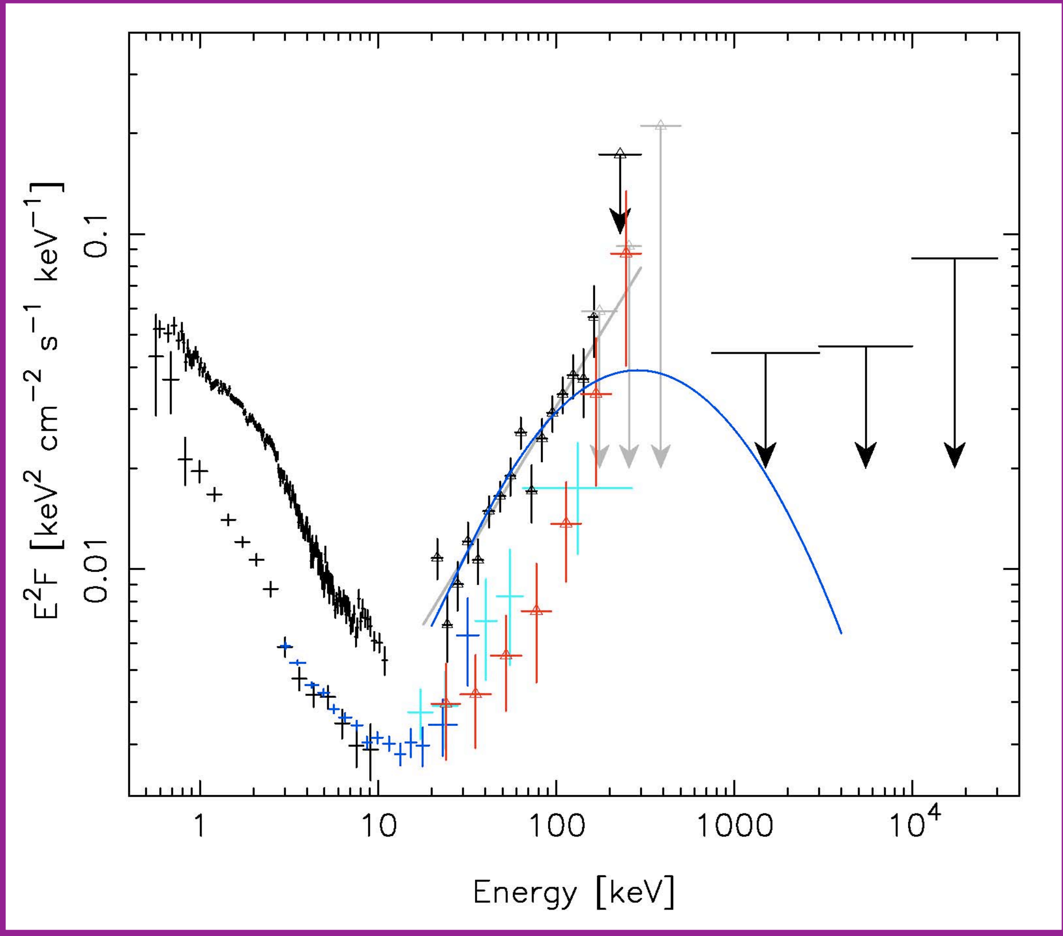

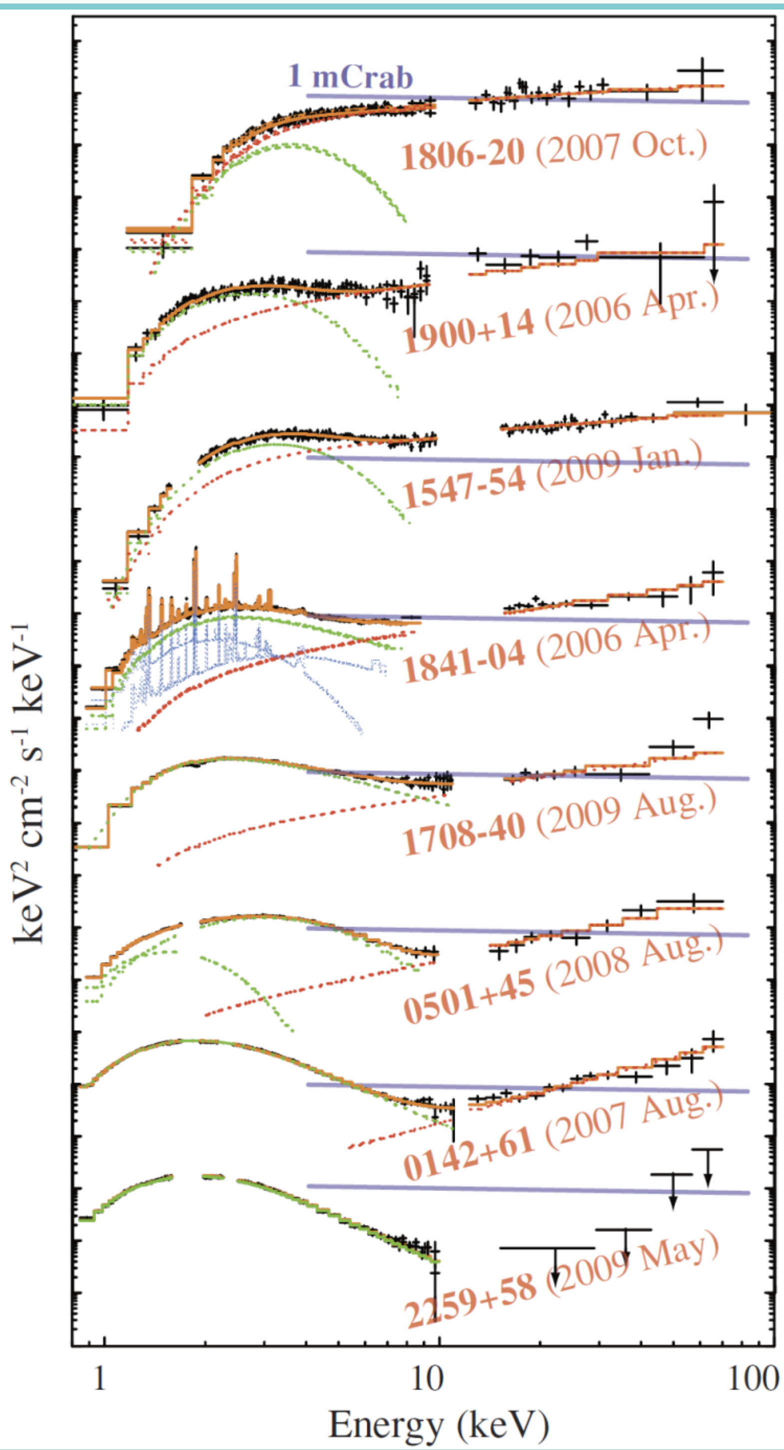

Enoto et al. (2010)

Hard X-ray Tails are Common in Magnetars

- Classical X-ray band 1-10 keV for SGRs and AXPs from Chandra + XMM observations;
- INTEGRAL-IBIS/ISGRI spectra in 20-100 keV band has a range of indices, with $E^{-\Gamma}$ for Γ=0.4-1.9. Similar for NuSTAR.
- There is some minor variability of index Γ on long timescales *e.g. SGR 1806-20*.
- Not all tail flux is pulsed.

Magnetars with Hard X-ray Tails

Table 1. Persistent Emission Spin-Down and Spectral Parameters for Magnetars with Hard X-ray Tails

Pulsar (a)	SNR	P (sec)	$\dot{P}$ (sec sec^{-1})	$\tau = P/2\dot{P}$ (kyr)	B_p (Gauss) (b)	B_p/B_{cr} (c)	$L_X/\lvert\dot{E}_{ROT}\rvert$ (d)	kT_b (keV)	Γ_s (e)	Γ_h (total) (f)	Γ_h^p (pulsed) (f)
SGR 1806-20	–	7.60	7.5×10^{-10}	0.16	4.8×10^{15}	110	6.2	$0.6^{+0.2}_{-0.1}$	$1.6^{+0.1}_{-0.3}$	1.7 ± 0.3	–
SGR 1900+14	–	5.20	9.2×10^{-11}	0.90	1.4×10^{15}	32	14	0.47 ± 0.02	1.9 ± 0.15	1.9 ± 0.3	–
AXP 1E 1841-045	Kes 73	11.78	$\sim 4 \times 10^{-11}$	4.7	1.4×10^{15}	31	880	0.450 ± 0.03	1.9 ± 0.2	1.32 ± 0.11	0.72 ± 0.15
AXP 1RXS J1708-40	–	11.0	1.9×10^{-11}	9.1	9.3×10^{14}	21	340	0.456 ± 0.009	$2.83^{+0.03}_{-0.08}$	1.13 ± 0.06	0.86 ± 0.16
SGR J1935+2154	G57.2+0.8	3.25	1.43×10^{-11}	3.6	4.4×10^{14}	9.9	1.3	0.46 ± 0.01	$2.4^{+0.4}_{-0.6}$	0.9 ± 0.1	–
SGR J1550-5408 [a]	G327.24-0.13	2.07	2.2×10^{-11}	1.5	4.3×10^{14}	9.8	> 0.008	$0.43^{+0.03}_{-0.04}$	$3.7^{+0.8}_{-2.0}$	1.54 ± 0.05	–
SGR 0501+4516	–	5.76	5.8×10^{-12}	16	3.7×10^{14}	8.4	–	–	–	0.7 ± 0.3	–
AXP 4U 0142+61	–	8.69	2.0×10^{-12}	69	2.7×10^{14}	6.0	2900	$0.410^{+0.004}_{-0.002}$	3.88 ± 0.01	0.93 ± 0.06	0.4 ± 0.15
AXP 2259+586	CTB 109	6.98	4.8×10^{-13}	230	1.2×10^{14}	2.7	> 390	0.412 ± 0.006	3.6 ± 0.1	0.8 ± 0.3	–

Tail index

From Wadiasingh et al. (2019, in prep.)

Hard X-ray Tail Modeling

- Preferred hypothesis is the resonant Compton upscattering model (Baring & Harding 2007; Fernandez & Thomson 2007; Nobili, Turolla & Zane, 2008; Baring, Wadiasingh & Gonthier 2011, Beloborodov 2013, and later papers):
  - non-thermal hard X-rays are spawned by inverse Compton heating of soft, atmospheric photons by relativistic electrons.
- The electrons are presumed to be accelerated probably along closed field lines, by static electric potentials, or dynamic ones associated with large scale currents and twists in the magnetic field (e.g. Thompson & Beloborodov 2005; Parfrey et al. 2013).
- Currents/charge densities along closed field lines far exceed Goldreich-Julian values;
- The putative locale of scattering is the inner magnetosphere, within 1-10 stellar radii of the surface.

Resonant Compton Cooling Geometry

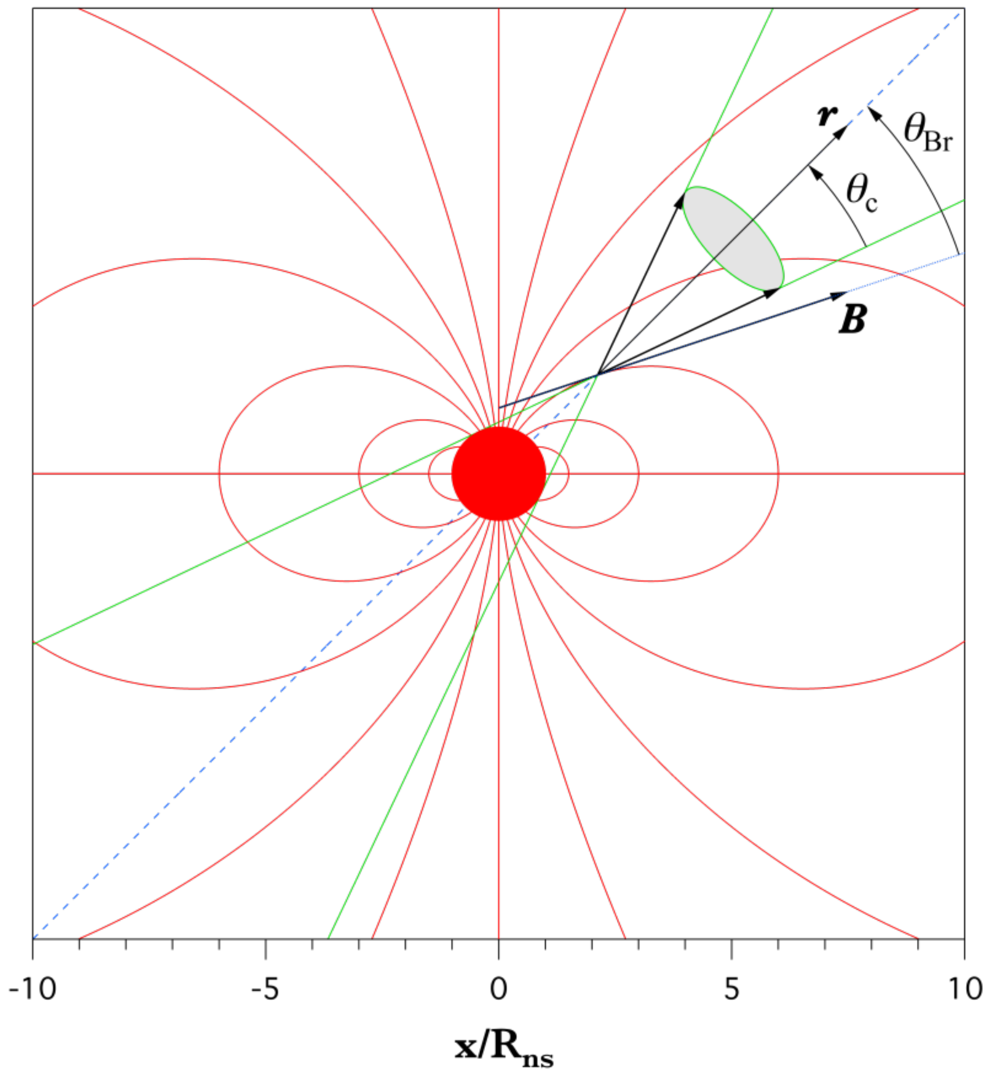

- Baring, Wadiasingh & Gonthier (2011) computed resonant Compton cooling rates for hemispherical soft photons in magnetospheric geometry.

Resonant Thomson Cross Section

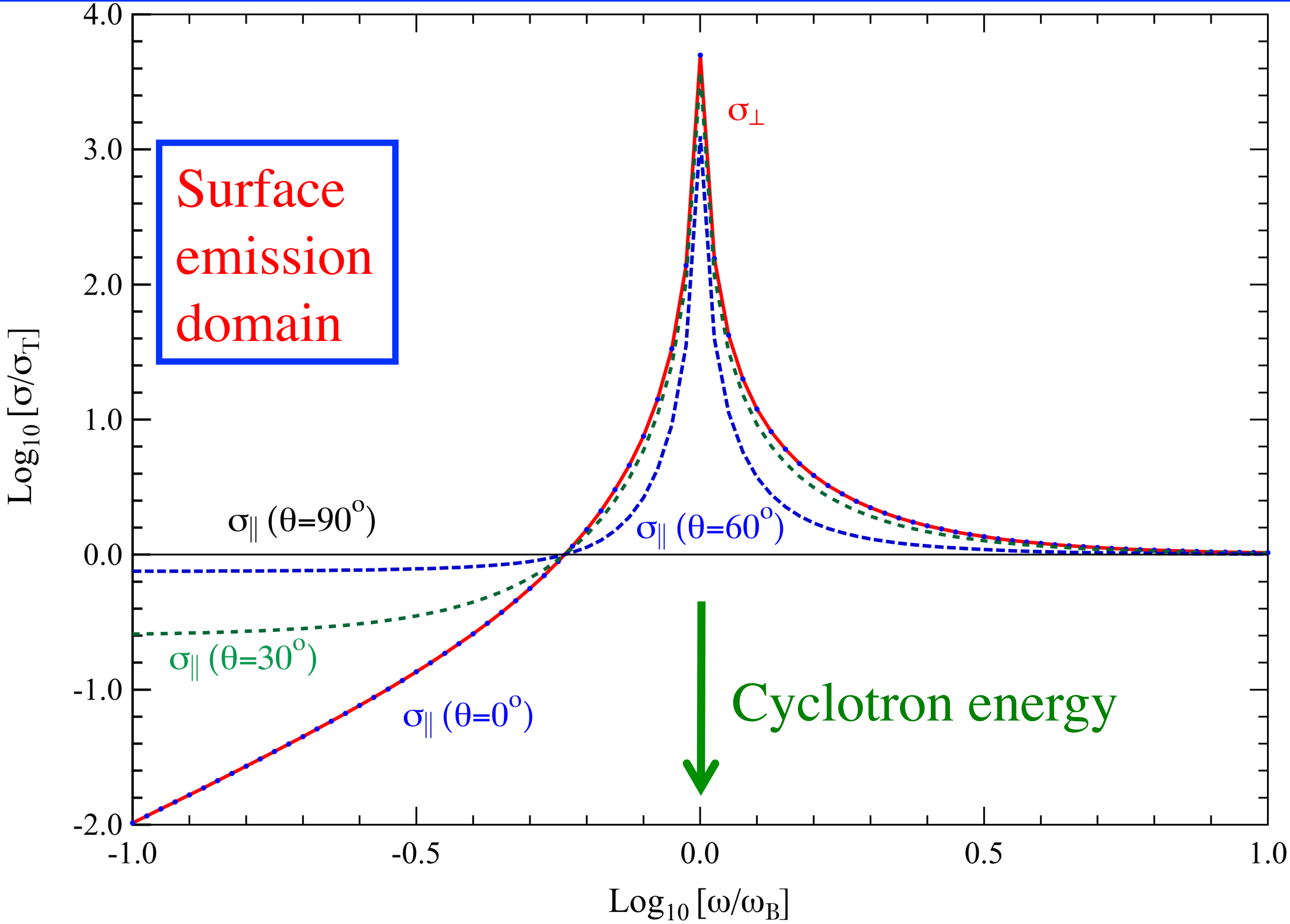

- Cross section of O-mode (| |) is strongly suppressed below cyclotron frequency ω_B for photons beamed almost along $\boldsymbol{B}$; same is true for X-mode (Canuto et al. 1971).

Resonant Compton Cross Section: QED

- Illustrated for photon propagation along **B**;
- In magnetar fields, cross section declines due to Klein-Nishina reductions;
- Resonance at cyclotron frequency eB/m_ec;
- Below resonance, *l=0* provides contribution;
- In resonance, cyclotron decay width truncates divergence.

B=1 => B=4.41 x 10^{13}G

Gonthier et al. 2000

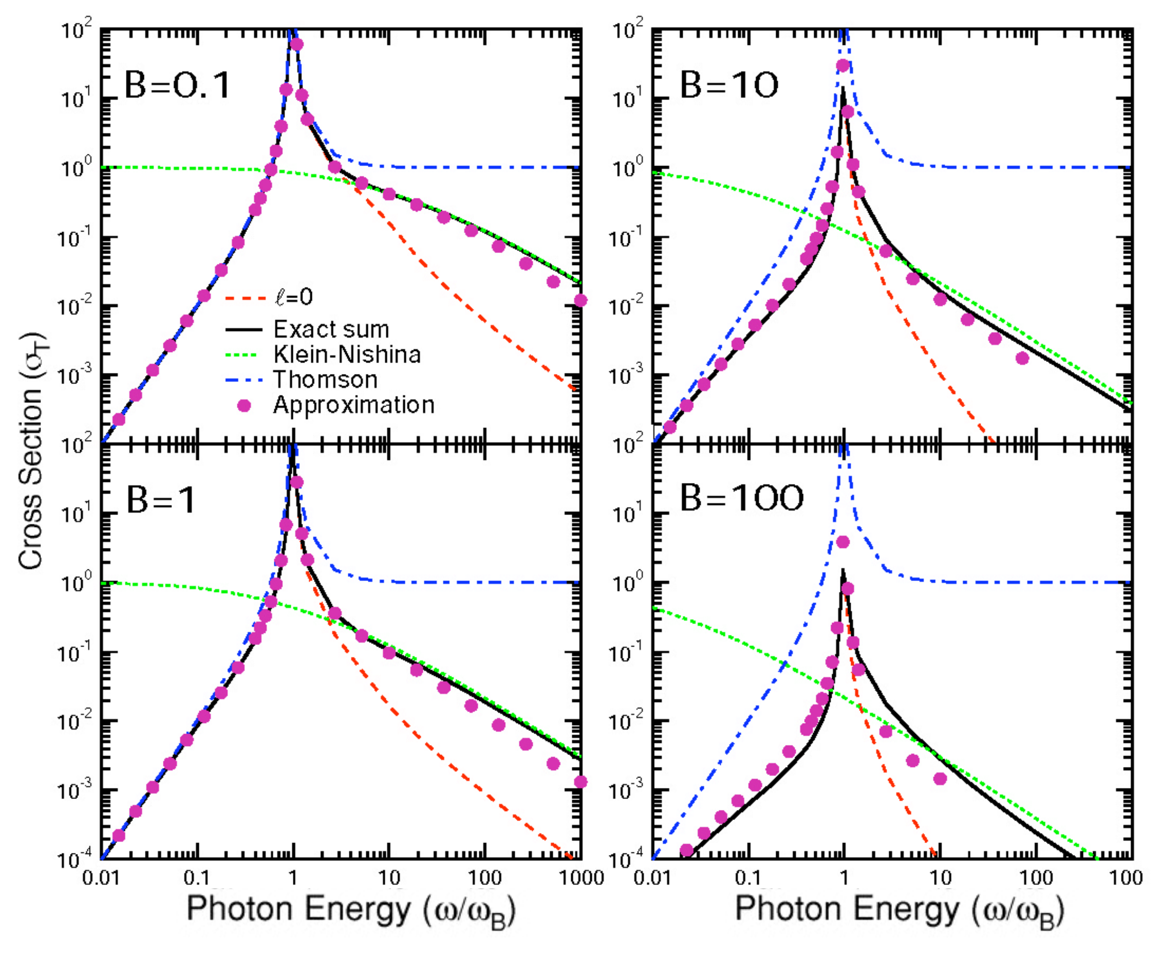

Process becomes effectively first order in the fine structure constant: the virtual electron behaves like a real one in the first excited state and spawns cyclotronic decay.

Resonant Interaction Geometry

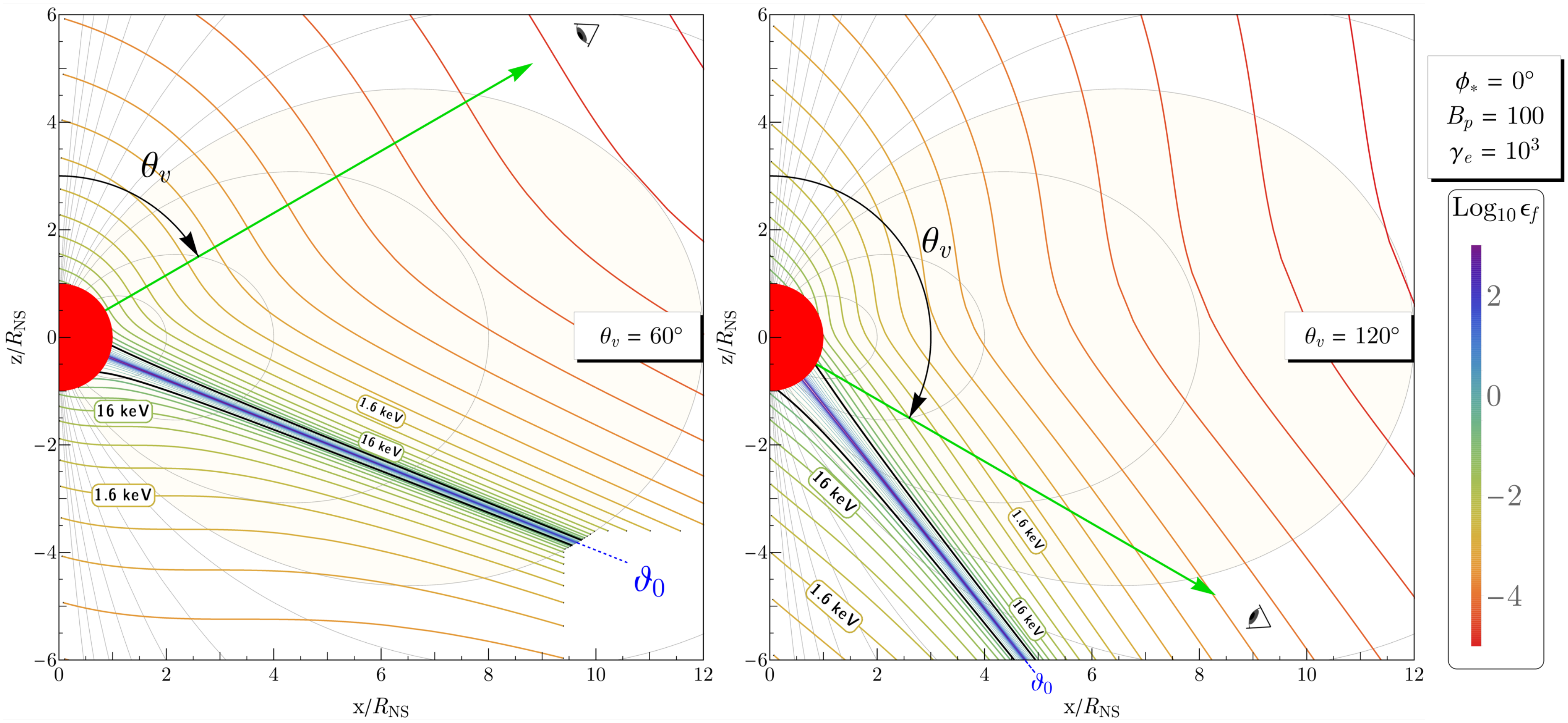

- Meridional case: hardest emission comes from concentrated zones of almost radial extension, with ***B*** directed toward observer.

Resonant Compton Emission Hardness: Dipole Fields

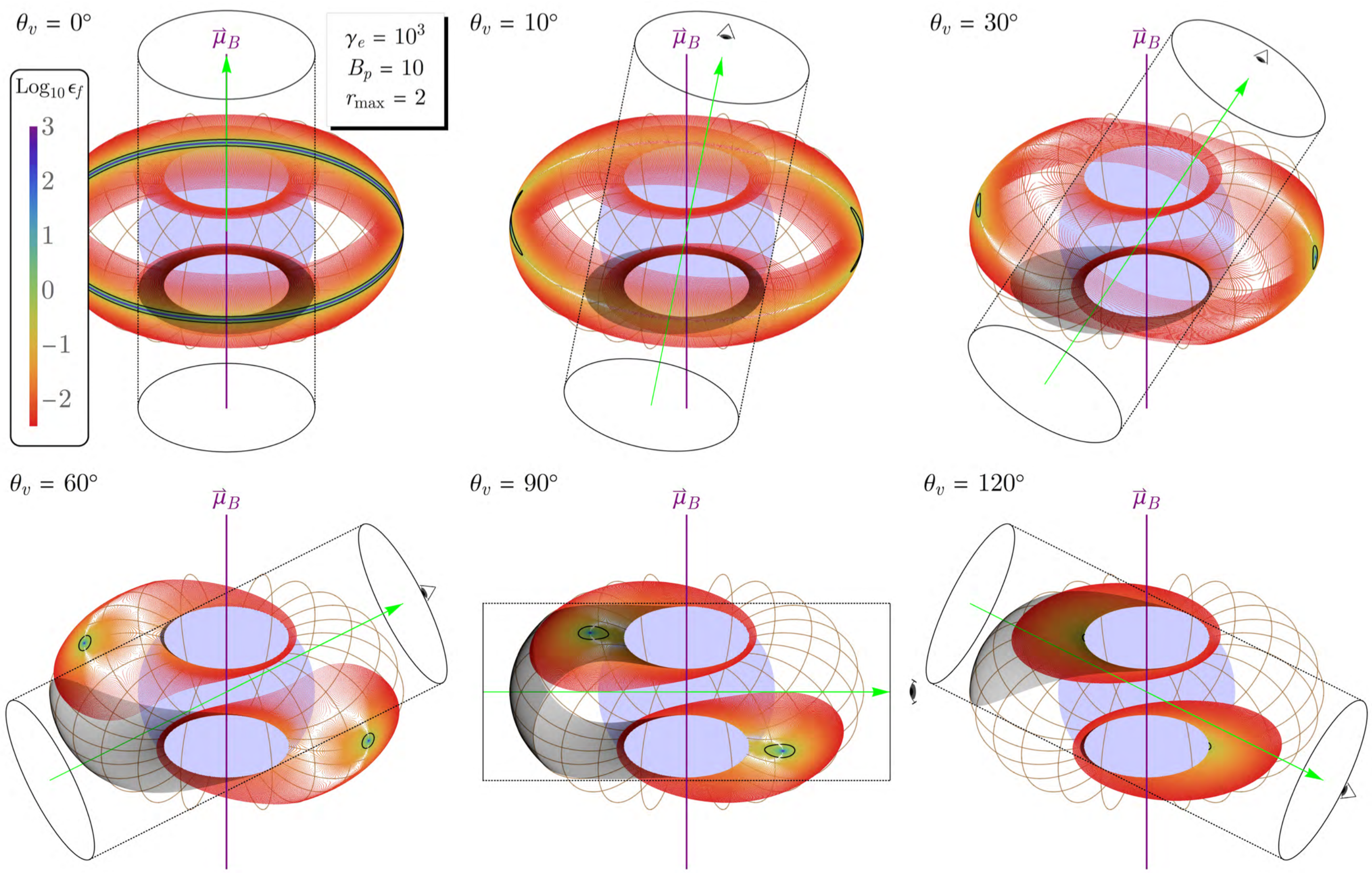

- Hard emission above 160 keV is blue or purple, softer emission is green or red.
- For most viewing angles, X-rays above 160 keV come from a very small portion of the activated magnetosphere for the Lorentz factor and polar field chosen above.

Resonant Compton Spectra: Viewing Oblique to Field Loops

$$\gamma\varepsilon_i(1-\beta\cos\theta_{kB,i}) \approx B \sim \gamma\varepsilon_f(1-\beta\cos\theta_{kB,f})$$

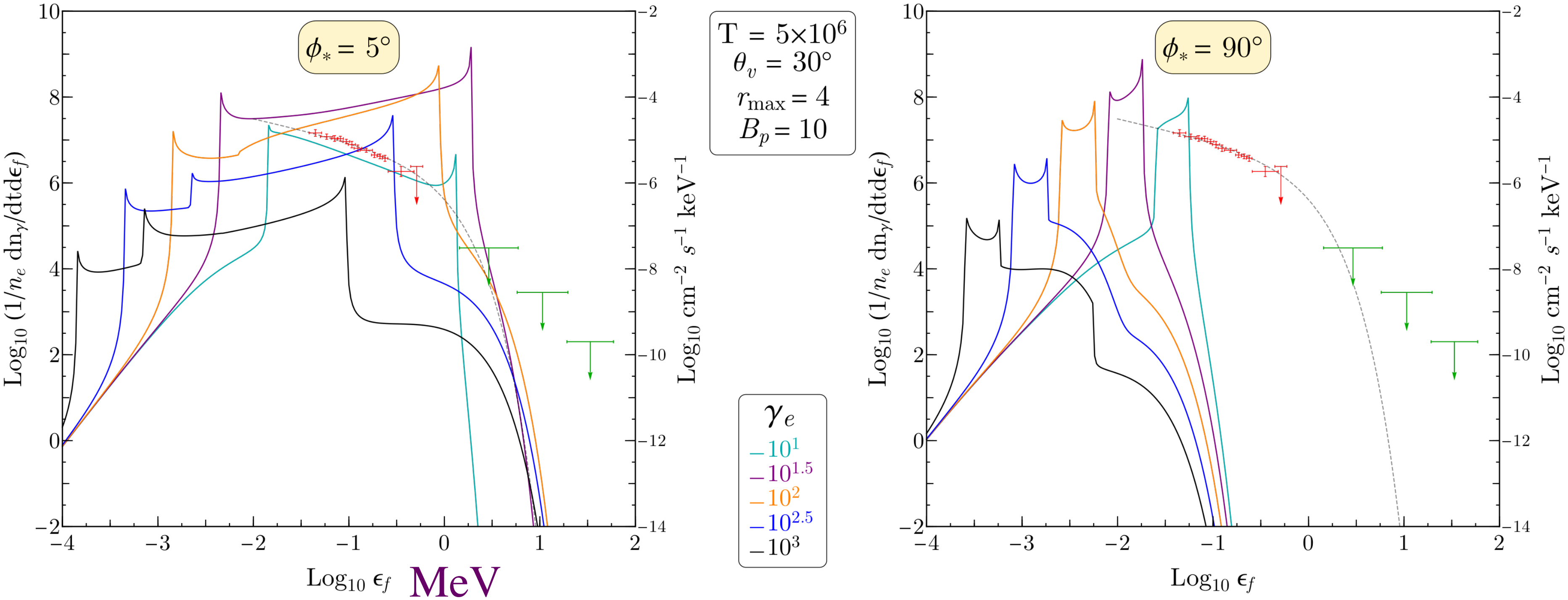

- Off-meridional field loops, varying γ_e: emission softer as Doppler boosting is less. (Wadiasingh et al., ApJ 2018). Guide spectrum: e.g. AXP 4U 0142+61.

Resonant Compton Spectra: Altitude Dependence from Loops

Wadiasingh et al.,
ApJ, 2018. [arXiv:1712.09643]

Photon splitting attenuates X-mode above ~50 keV.

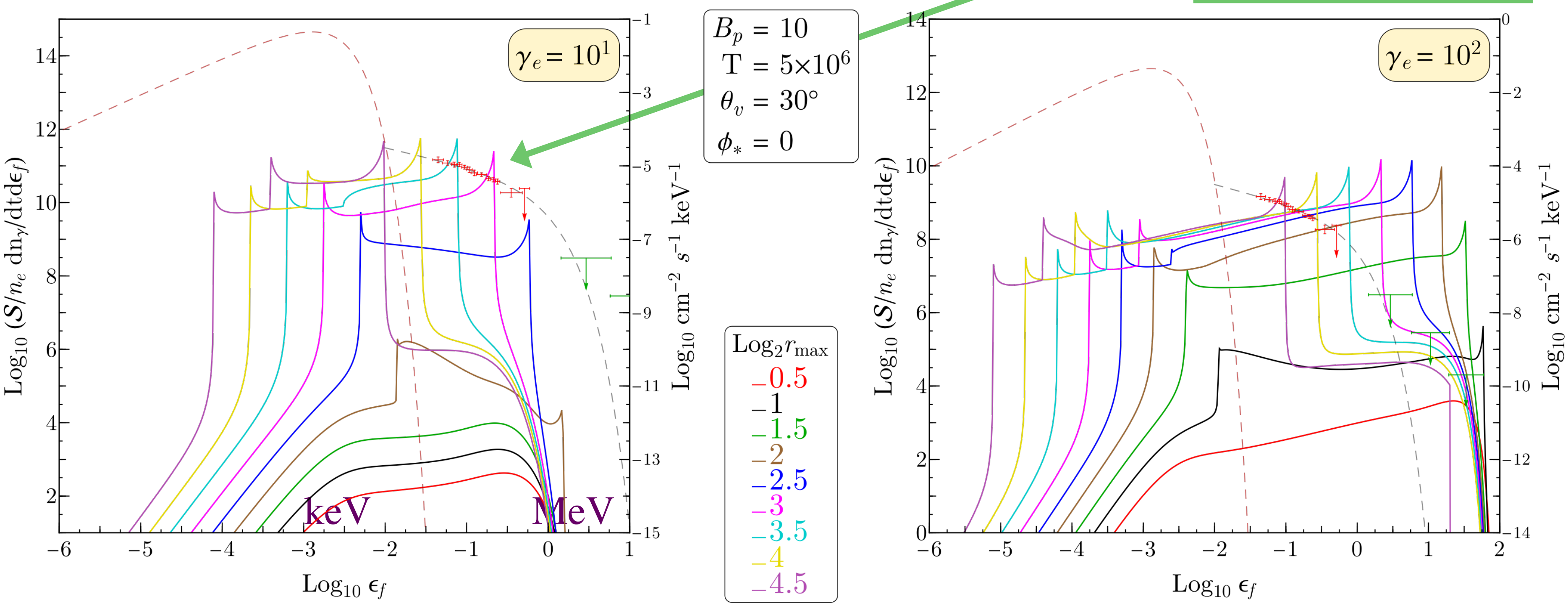

- Perpendicular (X-mode) exceeds parallel (O-mode) polarization at the highest energies; photon splitting will mute this above 50 keV.

Intensity "Sky maps" above 50 keV

Wadiasingh et al., in prep.

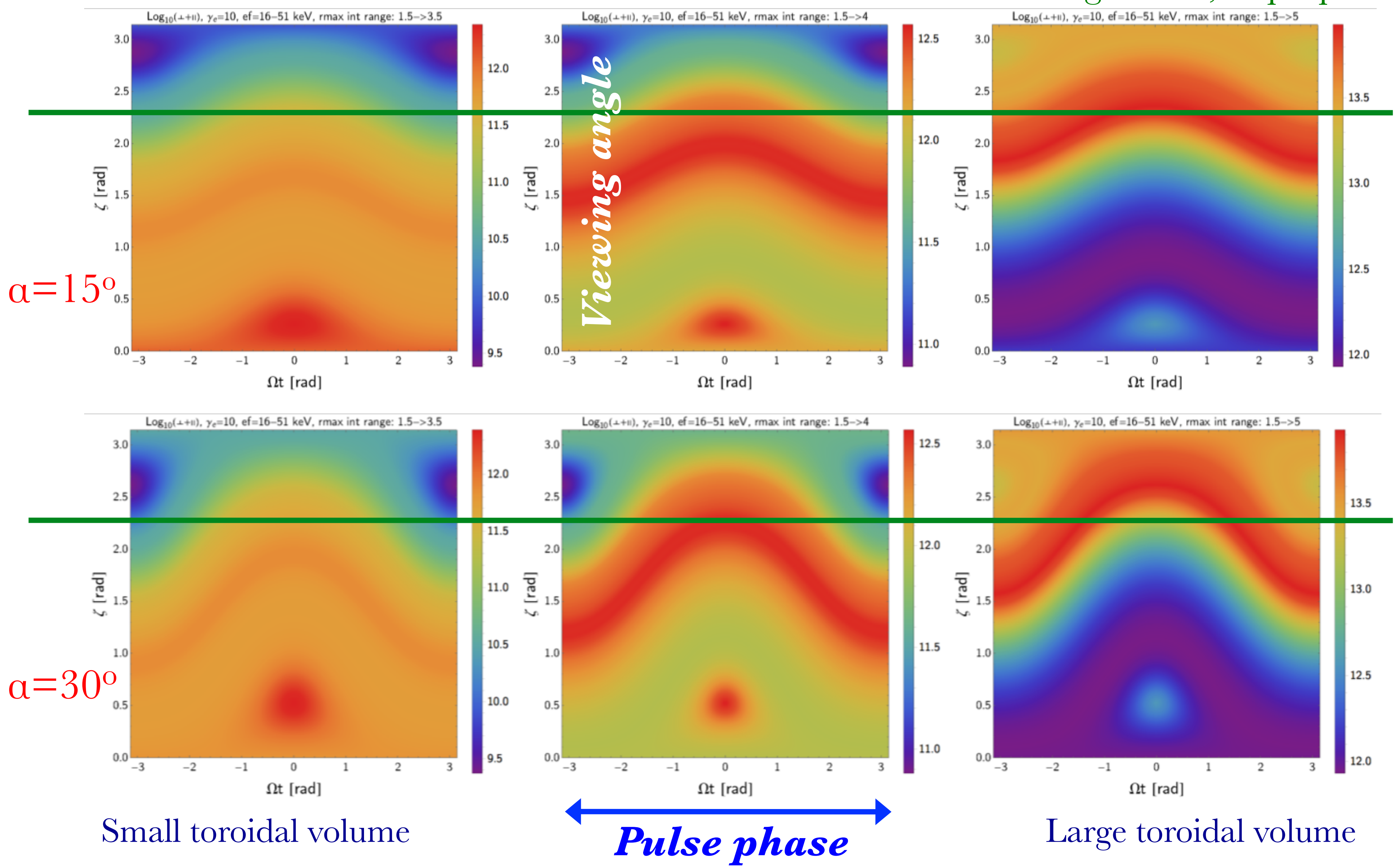

Small toroidal volume

Large toroidal volume

INTEGRAL/HEXTE Pulse Profiles of Magnetar J1708-4009

Kuiper et al. (2006)

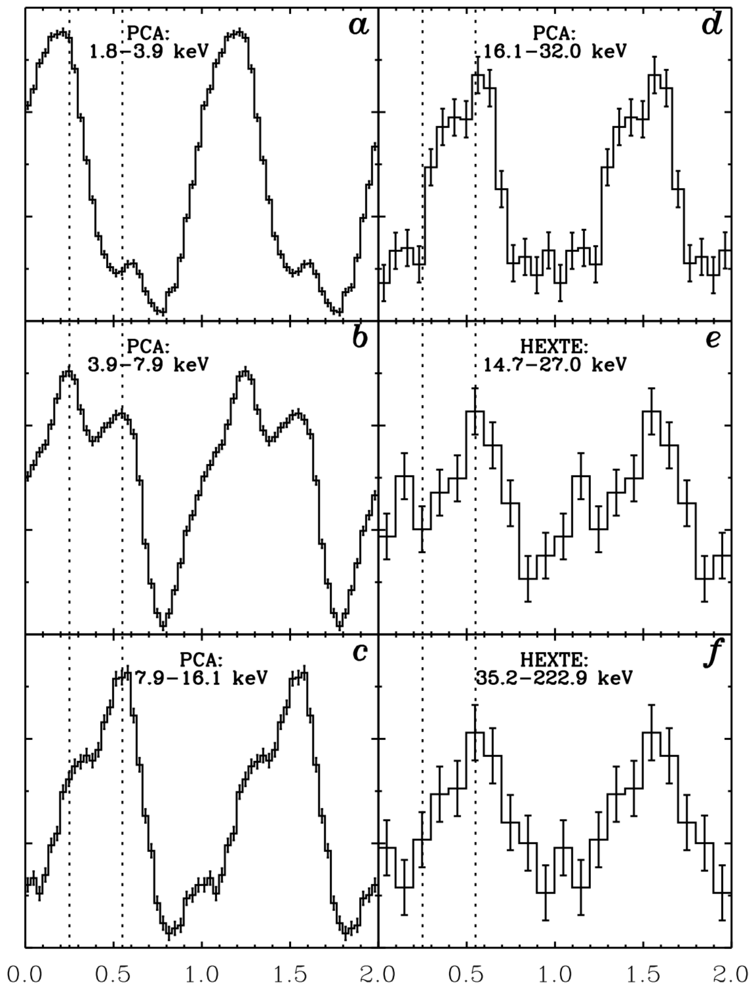

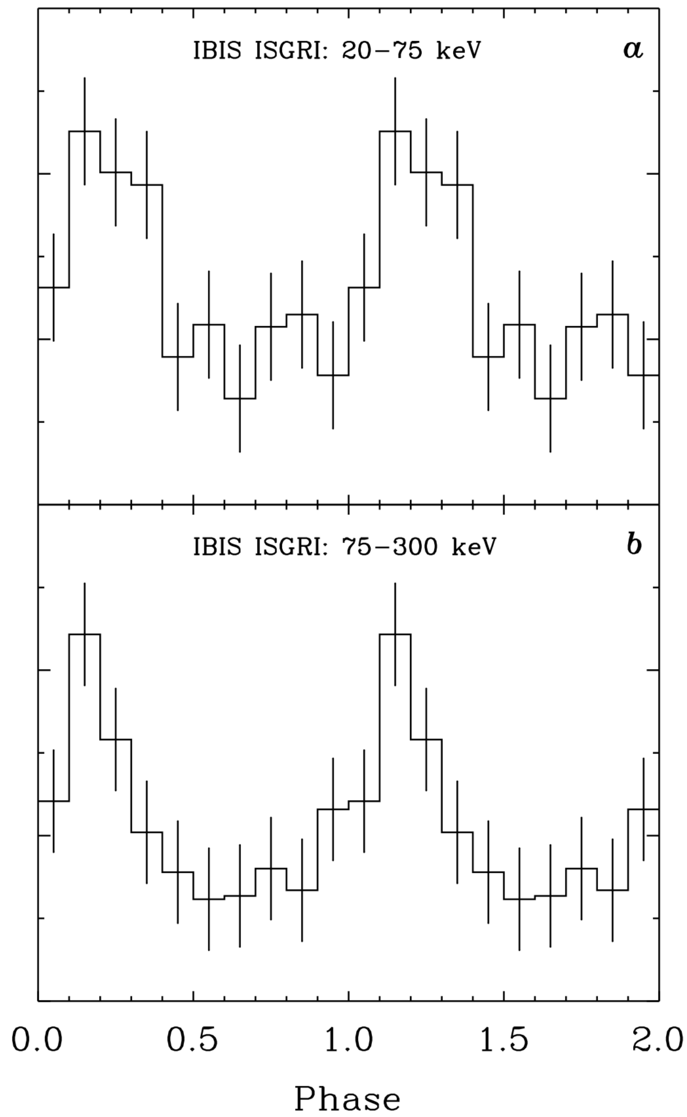

AMEGO Medium Energy Gamma-ray Telescope Concept

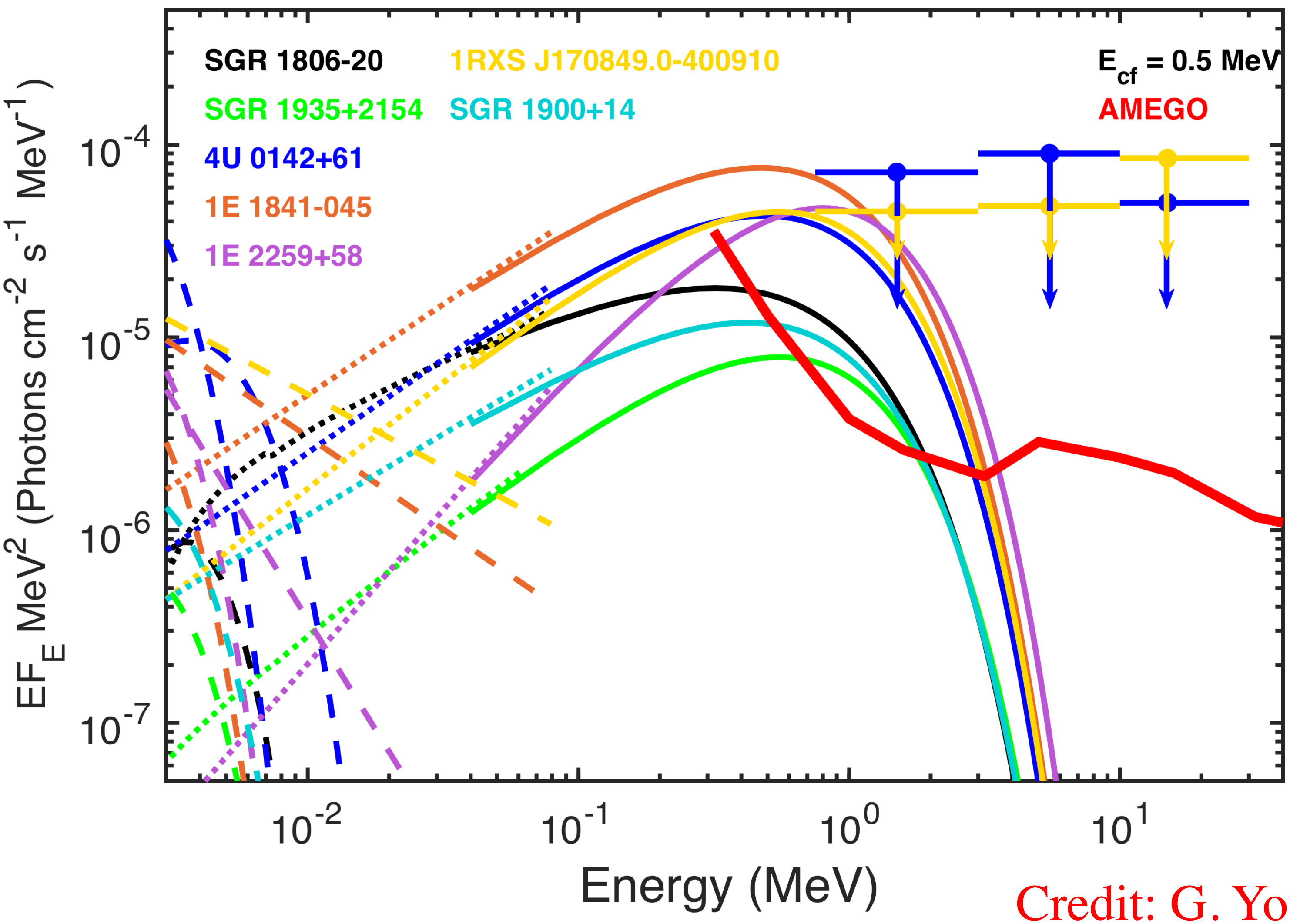

Credit: G. Younes

Spectro-Polarimetry Diagnostics

Wadiasingh et al. in prep.

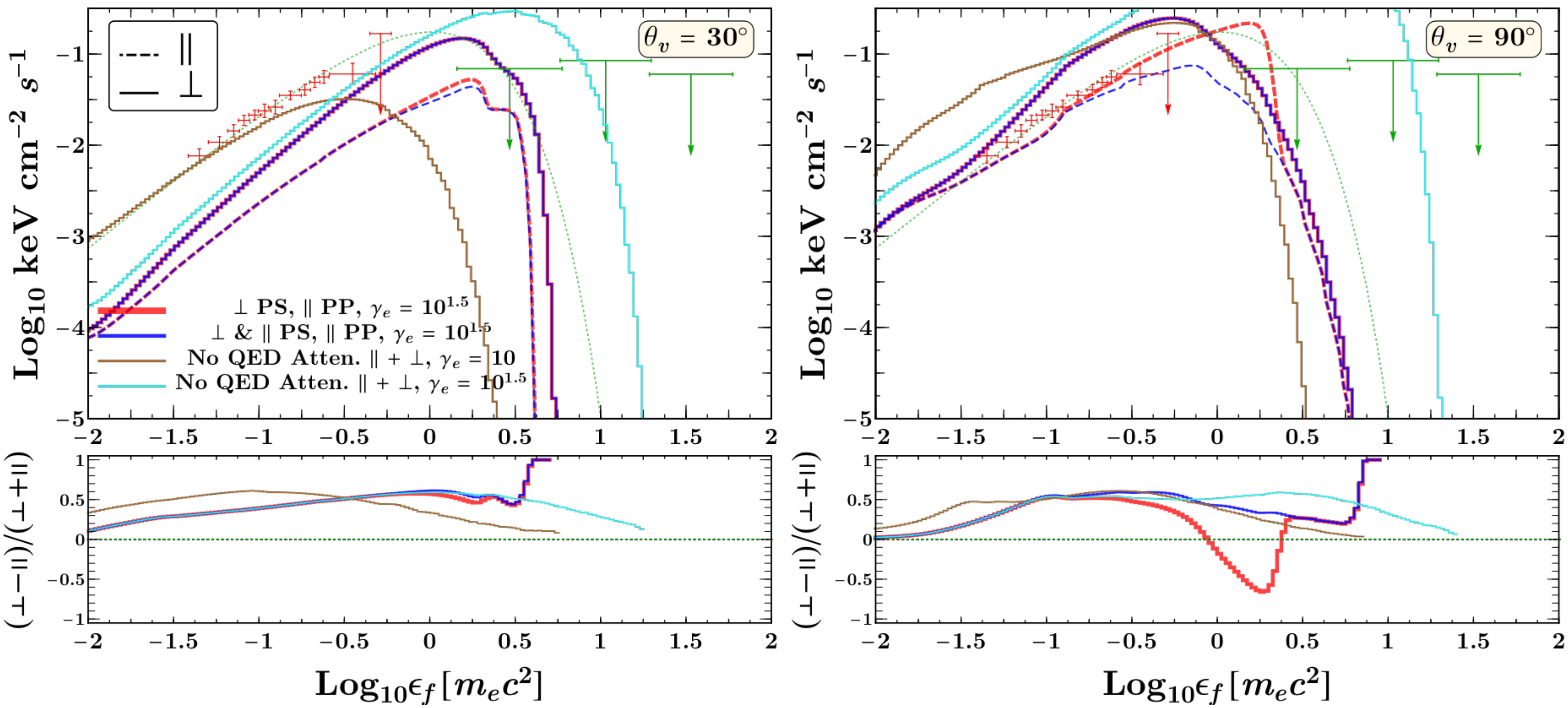

- Phase-resolved model RICS spectra of a generic magnetar with arbitrary normalization overlaid on phase-averaged data for 4U 0412+61. The inverse Compton emission is highly polarized and spin-phase dependent.

Conclusions

- Magnetic Compton upscattering can efficiently generate flat spectra like those seen in magnetar hard X-ray tails;
- Spectra are strongly dependent on observer perspective, electron Lorentz factor and emission locale;
- COMPTEL upper bounds can be met by large portions of the parameter space; they may also signal action of pair creation and photon splitting in attenuating spectra above 150 keV;
- Prospect: can use pulse profiles to probe values of magnetic inclination angle α of magnetars;
- Future agendas: Strong polarization signals above 50 keV prompt science agendas for Compton telescopes and polarimeters such as X-Calibur, AMEGO and e-ASTROGAM.